Sustainable Food Technology

ROYAL SOCIETY OF CHEMISTRY

PAPER

View Article Online
View Journal

Cite this: DOI: 10.1039/d5fb00942a

Lignocellulose nanofibers (LCNFs) reinforced starch-based intelligent film to detect chicken breast spoilage

Afreen Sultana,[a] Sneh Punia Bangar *[ab] and William Scott Whiteside*[a]

This study developed pH-sensitive starch-based films reinforced with peach pit-derived lignocellulose nanofibers (LCNFs) and blueberry anthocyanins (BA) at varying concentrations (0%, 10%, 25%, and 50%) for intelligent packaging of chicken. Anthocyanin was extracted from blueberries using acidified solvent extraction and incorporated into a starch/LCNF matrix to form films through solvent casting. The films were examined for their structural properties. Scanning electron microscopy (SEM) analyses confirmed that BA was successfully incorporated and uniformly dispersed within the starch/LCNF matrix. The tensile strength of the starch/LCNF/BA50 film was decreased by a factor of 4, while the elongation at break was increased to 12 times that of the control. Further, the color changes of films from reddish-pink at acidic pH (2) to greenish-yellow under alkaline conditions (pH 13) confirmed the excellent pH sensitivity of BA. Among all the tested films, the starch/LCNF/BA50 formulation, containing 50% BA, demonstrated the most sensitive color responsiveness. Additionally, the starch/LCNF/BA50 films exhibited strong antioxidant activity, with a DPPH radical scavenging rate of 53%. These films were subsequently used for intelligent chicken packaging under both ambient and refrigerated conditions. On the 10th day of storage (at 4 ± 1 °C), the pH and TBARS values of the chicken were recorded as 6.93 and 1.43 mg MDA per kg, both of which are indicative of significant lipid oxidation. Correspondingly, the starch/LCNF/BA50 film showed a significant color change from red to grayish-purple, further confirming its responsiveness to biochemical changes during spoilage. The developed pH-sensitive films could serve as effective indicators for monitoring freshness, supporting their potential use in intelligent food packaging systems.

Received 15th December 2025
Accepted 11th March 2026

DOI: 10.1039/d5fb00942a

rsc.li/susfoodtech

Sustainability spotlight

This research advances sustainable food technology by adding value to waste in the food processing industry. A typically discarded byproduct of the peach processing industry is converted into a stable, functional ingredient through a combination of chemical and mechanical treatments. During processing, peaches produce a lot of by-products, which include peel, stone (seed shell and seed), and pomace. The study contributes to waste reduction and adds new value streams for the food and packaging industries by reusing waste from the agroindustry and contributing to the circular economy. Further investigation determines the effects of blueberry anthocyanin incorporation at varying levels on film characteristics and its application in food packaging. These research objectives are aligned with Clemson University's Sustainability Action Plan. This research could have potential benefits for the food packaging industry.

1. Introduction

Lipid oxidation is a complex process in which fatty acids react with oxygen through the free radical mechanism. As a result, hydroperoxides are produced, which are odorless but extremely unstable. They quickly decompose into secondary chemicals, such as acids, alcohols, esters, ketones, hydrocarbons, and aldehydes, which impart undesirable flavors and odors to meat.[1] Due to their high concentrations, low odor thresholds, and significant role in volatile flavors, aldehydes are the most important of these compounds. Some of the aldehydes that affect the nutritional and organoleptic qualities of proteins include *n*-alkanals, *trans*-2-alkenals, 4-hydroxy-*trans*-2-alkenals, and malondialdehyde.[2] Simultaneously, chicken breast spoilage leads to protein breakdown due to microbial growth, producing ammonia and amino acids.

Monitoring the freshness of meat products throughout the supply chain is essential to prevent serious health risks associated with the consumption of spoiled or contaminated food.[3] Traditional methods of assessing food freshness, including physicochemical, microbiological, and sensory evaluations, are often labor-intensive and time-consuming and frequently require specialized laboratory equipment and trained

[a]Department of Food, Nutrition and Packaging Sciences, Clemson University, Clemson, SC 29634, USA. E-mail: wwhtsd@clemson.edu

[b]Department of Packaging and Graphic Media Science, Rochester Institute of Technology, Rochester, NY, 14623, USA. E-mail: spbipk@rit.edu

personnel. As a result, they rarely provide real-time, reliable freshness information to producers, retailers, or consumers.[4]

To monitor meat spoilage, pH-sensitive dyes are developed that change color from acidic to basic forms due to volatile amines produced by meat decay. Therefore, pH-responsive colorimetric films, which change color in response to lipid oxidation and metabolic changes during spoilage, have emerged as viable tools for real-time food quality monitoring.[5] The pH-responsive film uses a color-reactive substance that reacts with the water molecules in the intelligent packaging to produce hydroxide ions when it detects a change in the pH of the packaging system caused by the accumulation of organic amines or basic nitrogenous compounds during the storage of meat.[6] The color-reactive substance (known as dye) can be synthetic (of chemical origin), like bromocresol purple, methyl red, and cresol red, or natural (derived from plants, animals, minerals, and microbes), like anthocyanins, curcumin, shikonin, alizarin, and betalain.[7] Natural dyes are preferred over synthetic dyes in an intelligent packaging system because migration of synthetic dyes can occur during the monitoring process, which can be carcinogenic.[8]

Anthocyanins, a key class of natural dyes, typically occur in six forms: malvidin, cyanidin, petunidin, peonidin, pelargonidin, and delphinidin. When anthocyanins are exposed to a high concentration of hydroxyl groups or at a high pH, their electrons become delocalized, resulting in a color change. Due to their sensitivity to pH, these chemicals can react with volatile compounds emitted from meat spoilage, altering their structure, resulting in a color change and predicting the quality.[9,10] Blueberries, often called the "king of anthocyanins," contain the highest concentrations, around 7 mg per g dry matter.[11,12] Several studies have developed intelligent starch-based films incorporating blueberries in different forms, including blueberry extract,[3,13] blueberry peel,[14] blueberry powder,[15] and blueberry residue.[16]

Andretta *et al.*, 2019 employed the thermocompression technique to develop cassava starch-based films containing 10% blueberry residue (w/w, based on the starch content). These films exhibited a reddish-orange color at acidic pH values (2–5) and shifted toward a yellowish-green color at basic pH values (6–12). However, the thermocompressed films exhibited a decrease in tensile strength from approximately 6 MPa to 4 MPa, accompanied by a 35% increase in elongation at break.[16] In one study, ethanol-dissolved blueberry extract (up to 3% w/w) was sprayed onto starch/poly(butylene adipate-*co*-terephthalate) (PBAT) pellets prior to extrusion blowing. The resulting films exhibited enhanced antibacterial activity (72.40%), antioxidant capacity (68.69%), and a tensile strength of 7.85 MPa.[3] Lignin (A-LNP) was used to nanoencapsulate blueberry anthocyanin, which was then utilized as an active ingredient in a polyvinyl alcohol (PVA) and polyethylene glycol (PEG) matrix for room-temperature packaging of tomatoes. On the 15th day of storage, tomatoes packed in PVA and PEG matrix lost 16% of their weight, while those packed in PVA and PEG matrix with A-LNP lost only 7%, indicating an increase in their shelf life.[17] The shelf-life of raw peeled shrimp was increased by 2 days by employing electrospun gelatin-xanthan gum mats containing 7% black barberry anthocyanin, because of the anthocyanin, which delayed lipid oxidation.[18] Commercially available products such as "FreshTag" and Toxinguard® are on the market for detecting spoilage and giving real-time information to consumers.[19] This research could be useful for providing sustainable, biodegradable alternatives to market available freshness indicators.

Building on this, our research group previously reported that reinforcing LCNFs into a starch matrix significantly improved mechanical properties and hydrophobicity. Therefore, the primary objective of the current study is to extract anthocyanins from blueberries and incorporate them into a starch–LCNF matrix to develop a pH-sensitive film. The second objective is to evaluate the colorimetric response of these films as indicators of chicken quality deterioration during storage at 4 °C ± 1 °C and 23 °C ± 1 °C.

2. Materials and methods

2.1. Materials

Blueberry was purchased from the supermarket (Food Lion) supplied by Naturipe Farm in Florida, United States. Peach pits were supplied by Titan Farms, Ridge Spring (South Carolina, United States), and pearl millet grains were bought from the USDA-certified B&B Organics brand. Sodium chlorite (80% pure, $NaClO_2$), sodium hydroxide (NaOH), sodium metabisulfite, and 95% ethanol were purchased from Thermo Fisher Scientific. Hydrochloric acid (HCl), 2-thiobarbituric acid, 2,2-diphenyl-1-picrylhydrazyl (DPPH), and sulfuric acid-ACS reagents (95–98%) were all acquired from Sigma Aldrich. Trichloroacetic acid was purchased from Macron Fine Chemicals.

2.2. Anthocyanin extraction from blueberry

Blueberries were washed, lyophilized (at −23 °C and 500 mTorr pressure with secondary drying temperature of 25 °C) using a freeze-drier (Harvest RightTM, Utah, USA), and then ground. Subsequently, 10 g of ground blueberry was macerated with 80 ml of 70% ethanol (v/v), and the pH of the solution was adjusted to 2 using 1 M HCl. The solution was refrigerated for 24 hours and then filtered using rWhatman filter paper No. 1 *via* vacuum filtration. Further, the solution was centrifuged at 5000×*g* for 10 minutes to obtain pure ethanolic anthocyanin filtrate. A rotary evaporator (IKA Rotary evaporator RV 10 D S99, USA) was then used to remove the solvent at 50 °C in the dark. The resulting extract coded as BA was kept at 4 ± 1 °C in the dark until it was needed. The streamlined flowchart shown in Fig. 1 was used to extract anthocyanins from blueberries.

2.3. pH-sensitive film preparation

Starch was isolated from pearl millet using the wet milling process, as described elsewhere.[20] LCNF was isolated from peach pits using a method involving four steps. This process involved bleaching of ground peach pits with $NaClO_2$, alkali treatment with NaOH, and mechanical fibrillation using a planetary ball mill, followed by ultrasonication to yield nanoscale fibers.[21]

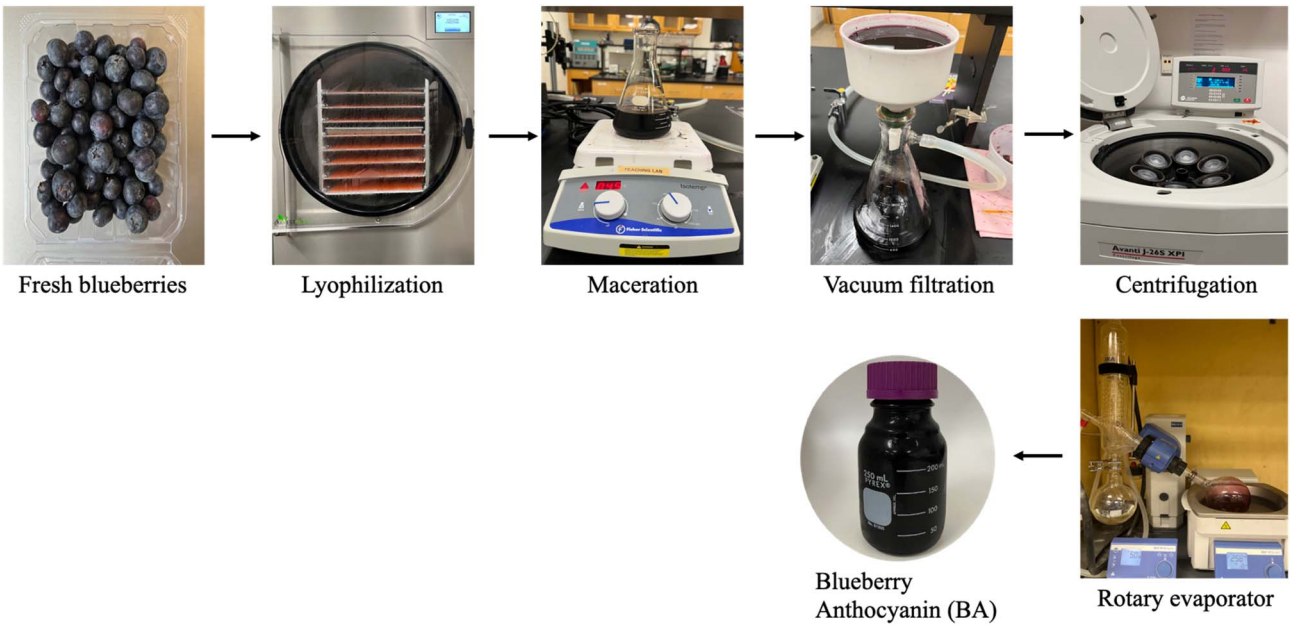

Fig. 1 Schematic representation of the step-by-step procedure for the extraction of anthocyanins from blueberries.

Based on the results of our previous research, we selected the film formulation with the best mechanical and water-barrier properties. In 50 ml of distilled water, pearl millet starch (3 g) and glycerol (30% of the starch weight) were added to prepare a starch slurry. In the remaining 50 ml of distilled water, 1.66% (w/w) of the LCNF was well-dispersed to form the LCNF suspension using ultrasonication (40% amplitude, 30 minutes). Further, LCNF suspension is added to the starch slurry to make up 100 ml of film-forming solution. The solution was homogenized for 5 minutes, followed by stirring at 400 rpm for 1 hour at 80 °C. Further, the film-forming solution was cooled to 50 °C, and 0%, 10%, 25% and 50% (of starch weight) of BA was added to develop pH-sensitive LCNF-reinforced starch-based films and coded as starch/LCNF/BA0, starch/LCNF/BA10, starch/LCNF/BA25, and starch/LCNF/BA50 (Table 1). Approximately 60 ml of the homogeneous solution was poured into polystyrene Petri dishes (150 mm in diameter) and left to dry in a hot-air oven at 50 °C for 48 hours. The thickness of the prepared films was measured using a digital micrometer (Excel Technologies, Inc., Arizona, USA) at five random points for each film sample. The starch/LCNF/BA0, starch/LCNF/BA10, starch/LCNF/BA25, and starch/LCNF/BA50 films exhibited average thicknesses of 4.02 ± 0.08 μm, 4.05 ± 0.10 μm, 4.08 ± 0.07 μm, and 4.12 ± 0.09 μm, respectively. No statistically significant differences were observed among the films ($p > 0.05$). No statistically significant differences were observed among the films ($p > 0.05$), indicating that incorporation of anthocyanins up to 50% did not affect film thickness.

2.4. pH sensitivity and UV-vis spectral analysis of BA

In 9 ml of a buffer solution with a pH range of 2 to 13, 1 ml of BA was dissolved. Pictures of the solutions were captured. UV-visible spectroscopy is used to measure the absorbance of BA, assessing how its color changes in response to various pH solutions. These absorption spectra of the solution in the 400–800 nm region were captured using a Spectronic Genesys 20 spectrophotometer.

2.5. Color measurement of films

The change in color for the prepared films with varying BA content (10%, 25%, and 50%) at various pH levels was

Table 1 Composition of control and starch/LCNF/BA films with different BA concentrations

Sample	Starch (3% w/v) (g)	Glycerol (30% of starch) (ml)	LCNF suspension (0.1%)	LCNF concentration as per the starch (%)	LCNF concentration in grams (g)	BA concentration (ml)	Total volume (ml)
Starch/LCNF/BA0	3	0.9	50% – 50 ml	1.66	0.050	0	100
Starch/LCNF/BA10	3	0.9	50% – 50 ml	1.66	0.050	0.3	100
Starch/LCNF/BA25	3	0.9	50% – 50 ml	1.66	0.050	0.75	100
Starch/LCNF/BA50	3	0.9	50% – 50 ml	1.66	0.050	1.5	100

measured. Films were cut into 3 × 1 cm^2 rectangular strips and submerged in buffer solutions with pH values ranging from 2 to 13 for 10 minutes. The films were then removed from the buffer solutions. Each film's images were captured using an iPhone 13. The color of the starch/LCNF/BA10, starch/LCNF/BA25, and starch/LCNF/BA50 films corresponding to a specific pH was determined using a HunterLabTM Aeros Spectrophotometer (Reston, VA) in three replicates. The values of the three-color parameters, l, a, and b, were measured where l stands for the sample's lightness (+) or darkness (−), a for its redness (+) or greenness (−), and b for its yellowness (+) or blueness (−). Using the following formula, the total color difference (ΔE) was determined:

$$\Delta E = \sqrt{(l^* - l)^2 + (a^* - a)^2 + (b^* - b)^2}$$

where l^*, a^*, and b^* values represent the values of the films before submerging into pH buffers.

2.6. Microscopic structure of films

The film pieces were adhered to a metal stage using double-sided tape, and then sputter-coated with platinum for 3 minutes to increase their conductivity. With a High-Resolution Scanning Electron Microscope-Regulus 8230 (Hitachi High Technologies America, Inc., United States) set to 9000× magnification and 5 kV acceleration voltage, the surface morphologies of the film samples were examined.

2.7. Chemical structural analysis

To analyze the changes in the chemical structure of the pH-sensitive films compared to control films, Fourier transform infrared spectroscopy (FTIR) was used to record the spectra of the films using Thermo Fisher Scientific's Nicolet iSTM 10 FTIR spectrometer (United States). With a resolution of 4 cm^{-1} over the wavenumber range of 4000–500 cm^{-1}, the instrument was run in the attenuated total reflectance (ATR) Fourier transform mode.

2.8. Mechanical strength

The ASTM-D882 standard was used to evaluate the mechanical strength of control films and pH-sensitive film samples by measuring their tensile strength, elongation at break, and Young's modulus. A Universal Testing Machine (INSTRON, New Jersey, United States) equipped with a 1 kN load cell was used to describe each film specimen after it had been sliced into 10 cm × 1.5 cm strips. An initial clamp spacing of 50.8 mm and a crosshead speed of 10 mm min^{-1} were used for the analysis.

2.9. Thermal stability

The thermal characteristics of the control films and pH-sensitive film samples were determined by thermogravimetric analysis (TGA) under a nitrogen flow of 40 ml min^{-1}. Film samples were dried at 45 °C, and around 2–5 mg of the film was placed in the pan of AutoTGA 2950 (Model V5.4A, TA Instruments, Delaware, United States). The experiment was conducted at a heating rate of 10 °C min^{-1}, with the temperature ranging from room temperature to 600 °C.

2.10. Water vapor transmission rate

Water vapor transmission rates (WVTR) of control and pH-sensitive films were measured using Permatran-W 3/34 by Mocon (Ametek, Minnesota, USA) (complies with the standard ASTM F1249). With a test area of 1.13 cm^2, a 3 × 3 cm film sample was cut and sandwiched between two aluminum masks. The test conditions were 38 °C and 90% relative humidity. The mean of two parallel measurements was used to provide the results in g per 100 $inch^2$ per day.

2.11. Antioxidant property of films

The diphenyl picrylhydrazyl (DPPH) free radical scavenging method was employed to assess the antioxidant activity of BA and the prepared pH-sensitive films. With this procedure, 10 ml of freshly prepared DPPH solution was mixed with 30 mg of film samples after the DPPH solution (0.01 mM) had been dissolved in 99.9% methanol. After 24 hours in a dark room, the solution without film and extract was considered blank. After measuring the solutions' absorbance at 517 nm using a UV-vis spectrophotometer (Spectronic Genesys 20), the percentage of DPPH scavenging activity was determined using the formula below:

$$\text{DPPH scavenging activity\%} = [(\text{Abs DPPH} - \text{Abs sample})/\text{Abs DPPH}] \times 100$$

where Abs DPPH represents the absorbance of DPPH and Abs sample represents the absorbance of the sample.

2.12. Application of films for monitoring chicken freshness

2.12.1. Packaging of chicken. The supermarket (Food Lion, Clemson, USA) supplied the fresh, skinless chicken breasts, which were delivered to the laboratory within one hour of purchase. Chicken pieces were cut into ∼80 g. Wax paper was placed inside the polypropylene container (18 cm × 9 cm × 4.5 cm), and chicken samples were placed on it, covered with a transparent lid. The pH-sensitive films (3 × 1 cm^2) were placed on the inner surface of a transparent plastic lid (which was not in direct contact with the chicken sample). The packed chicken samples were placed in refrigerated conditions at 4 ± 1 °C, 30% RH, and at room temperature, 23 ± 1 °C, 50% RH. Three samples were taken randomly for photo, thiobarbituric reactive substances (TBARS), and pH analysis every second day for both 4 ± 1 °C and 23 ± 1 °C conditions over 10 days.

2.12.2. pH measurement. Five grams of chicken breast were sliced up and mixed with fifty milliliters of purified water. Following that, a Thermo Fisher ScientificTM Orion Star A214 pH/ISE Meter (Waltham, MA) was used to measure the homogenate.

2.12.3. TBARS. TBARS were determined in triplicate for each sample as described by Oxford Biomedical Research (2008). Initially, 5 g of the chicken sample is homogenized with 10 ml of deionized water using a homogenizer. This is followed by mixing 1 ml of the homogenate with a thiobarbituric acid/

trichloroacetic acid (TBA/TCA) solution, then vortexing using a vortex mixer. The mixture is heated at 90 °C, and upon cooling, it is centrifuged using an Eppendorf 5804R centrifuge. After filtration through a 0.45 μm filter, absorbance is measured at 532 nm against a standard curve prepared with 1,1,3,3-tetrathoxypropane using a Spectronic® 20 GENESYSTEM™ spectrophotometer.

2.13. Statistical analysis

The data were recorded as the mean ± standard deviation, and differences among the samples were determined using a one-way analysis of variance (ANOVA) followed by Tukey's post hoc test. Statistical analysis was conducted using IBM SPSS Statistics software (version 28.2.0), with a significance level of $p < 0.05$. Triplicates (three independent samples) of the pH-sensitive film samples were considered for all the analyses.

3. Results and discussion

3.1. pH response and UV-vis spectrum determination of BA

Blueberry anthocyanins (BA) are natural pigments responsible for the vibrant red, purple, and blue colors of the fruit. The color variations of BA at various pH levels (2–13) and their light absorption behavior, measured using UV-vis spectroscopy, could be used to assess the viability of BA as a potential active component for preparing pH-sensitive films. Color changes in starch/LCNF/BA films were observed across pH buffer solutions. As illustrated in Fig. 2(a), these visual changes were clearly visible to the naked eye, indicating the responsiveness of BA within the film matrix to environmental pH. Anthocyanins possess the property of changing color, which is attributed to their diverse chemical structures and varies depending on the pH level, due to their ionic nature.[22] The buffer solution with BA ranged in color from reddish/pink to purple and then to yellow-green, during a change in pH from acidic to alkaline. A similar shift in color pattern from red to green was observed when blueberry peel extract was added to solutions with different pH levels, ranging from pH 2 to pH 10.[14] At pH 2, BA was a light red color, and gradually shifted to pink as the pH increased to 5. At neutral pH (7), the color changed to BA and then to light grayish blue as the environment became slightly alkaline. With a further increase in pH from 11 to 13, the BA solution changed to a greenish-yellow color. Likewise, Hu *et al.*, 2024 observed that blueberry-extracted anthocyanins appeared reddish-pink in acidic media, gradually turning purple, blue-violet, and eventually yellow-brown as the alkalinity of the solution increased.[23] These consistent observations confirm the strong pH responsiveness of BA, reinforcing its potential as a natural colorimetric indicator for intelligent packaging applications.

The UV-visible absorption bands of BA solutions varied with pH (Fig. 2(b)). In the visible portion of the UV-vis spectrum (400 nm to 700 nm), the BA solution displayed a bright red color in the strong acid environment (pH 2 and 3), along with the appearance of the maximum absorption peak (λ_{max}) at about 520 nm, primarily due to its molecular form of flavylium cation.[24] At pH 4, the solution exhibited a pink hue, and the intensity of λ_{max} decreased sharply, indicating a decrease in flavylium ion concentration. As the pH increased from 4 to 6,

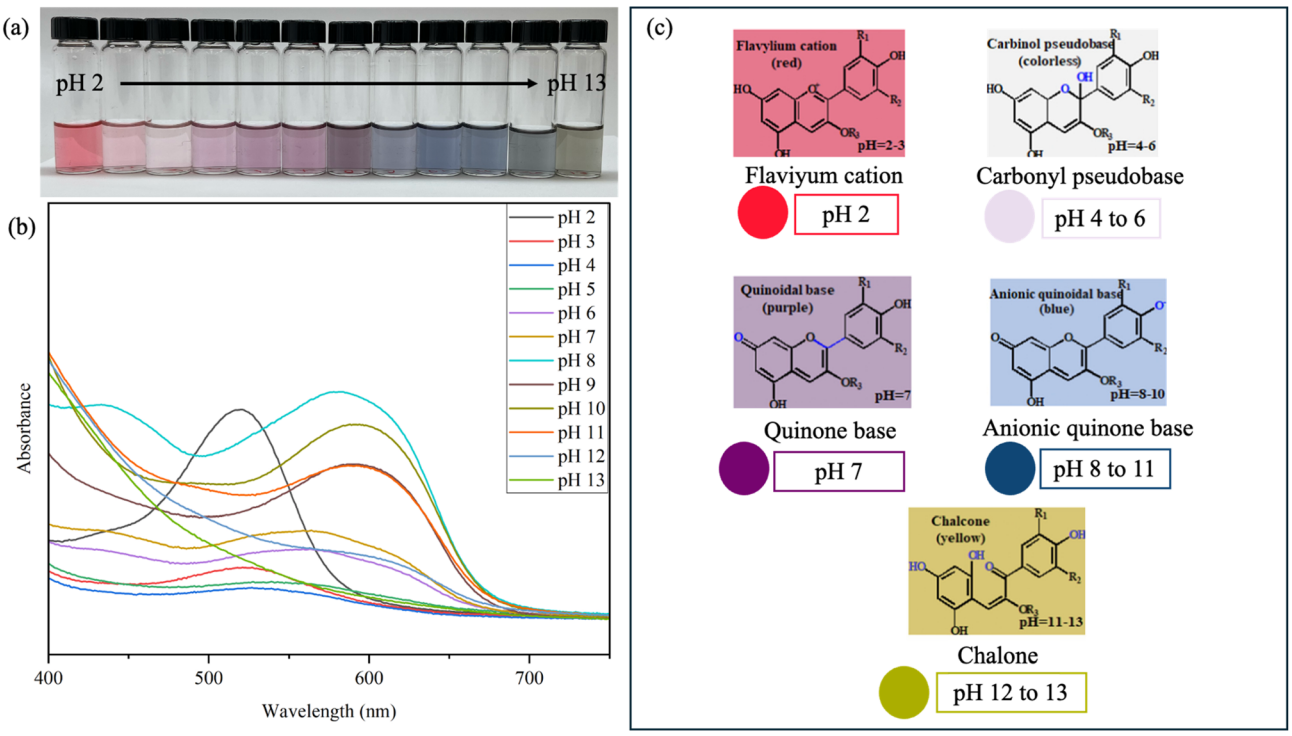

Fig. 2 (a) Shows the photos of BA in various pH buffers (2 to 13), (b) absorption spectra, and (c) structural changes of BA at pH solutions ranging between 2 and 13.

the solution gradually darkened, likely due to the accumulation of the colorless carbinol pseudobase due to the deprotonation of hydroxyl groups.[25] At neutral pH (7), the solution turned purplish, shifting further to a grayish-blue shade, which can be attributed to the presence of the quinonoidal base form.[26]

Under alkaline conditions (pH 8–11), the solution darkened further, with a slight increase in absorption intensity and a bathochromic shift of λ_{max} to approximately 590 nm. At higher alkalinity (pH 12–13), the absorption peak disappeared entirely, and the solution took on a brownish-yellow color, indicating the breakdown or transformation of anthocyanins into chalcone-like or degraded forms.[3]

The primary reason for the difference in the UV-visible absorption bands of anthocyanin solutions at varying pH values is the ability of anthocyanin molecules to absorb electromagnetic energy in the UV-visible spectrum.[27] Anthocyanins generally show distinct structures at different pH values: yellow salt ions (red in strongly acidic conditions), methanol pseudobases (colorless in weakly acidic conditions), quinone bases (blue in weakly alkaline conditions), and chalcone (yellow in strongly alkaline conditions).[28] Consequently, the structural alteration of anthocyanins at varying pH values is the primary source of the color shift and changes in the absorption peak. Taken together, these findings highlight the strong pH-responsive behavior of BA, demonstrating its potential as a natural dye for developing food freshness monitoring films that rely on clear and effective color changes in response to environmental pH.

3.2. Colorimeter changes in the film

Fig. 3 illustrates the pH responsiveness of the films. The starch/LCNF/BA0, which does not contain anthocyanins, showed no pH sensitivity and was therefore excluded from colorimetric analysis. On the other hand, anthocyanin-containing films, including starch/LCNF/BA10, starch/LCNF/BA25, and starch/LCNF/BA50, exhibited strong pH sensitivity and displayed noticeable color changes in various buffer solutions with pH values ranging from 2 to 13. Generally, as the pH level increased, the color of these films shifted from red to greenish yellow. Furthermore, increasing the anthocyanin content from 10% to 50% intensified the color changes, making the pH response more distinct and pronounced.

The L values of the films are shown in Fig. 4(a), and did not show a clear or consistent change with a change in pH. For starch/LCNF/BA10, L values ranged from 79.18 ± 1.1 (pH 2) to 80.42 ± 0.45 (pH 13). For starch/LCNF/BA25, L values ranged from 75.83 ± 1.2 (pH 2) to 74.71 ± 0.9 (pH 13). And for starch/LCNF/BA50, L values ranged from 69.23 ± 0.6 (pH 2) to 75.4 ± 0.6 (pH 13). Similarly, a film composed of 99% amylose and red cabbage anthocyanin was exposed to buffer solutions ranging from 2 to 11. The L values remained either non-significantly or only slightly affected between pH 2 and 8. However, a statistically significant increase in L value from 34.6 to 36.9 was observed between pH 8 and 10.[29] Overall, a slight increase in L value, indicating increased lightness, was observed as pH increased to 6. With a further increase in pH to 10, the films exhibited increased darkness, followed by another rise in lightness at pH 13. These L value trends correlate well with the visible color changes in the films, as illustrated in Fig. 3.

For all the films, a^* value decreased as the pH increased from 2 to 13, as represented in Fig. 4(b). At pH 2, a^* value of starch/LCNF/BA10, starch/LCNF/BA25, and starch/LCNF/BA50 was recorded as 11.9 ± 0.4, 15.3 ± 0.7, and 16.25 ± 0.7, respectively. Upon increasing the pH to 13, the a^* value decreased to −2.27 ± 0.4, −3.52 ± 0.2, and −3.04 ± 0.6, respectively. Similar results have been observed for starch, PVA, and blueberry peel-based film, where on increasing the pH from 2 to 8, the a value decreased from 5.65 to −2.49, respectively.[14] As observed in Fig. 4(c), with the increase in pH from 2 to 13, b^* values of the films increased from −10.57 ± 0.5 to −4.01 ± 0.3, −12.07 ± 0.7 to −1.57 ± 0.4 and −12.5 ± 0.7 to −0.8 ± 0.2 for starch/LCNF/BA10, starch/LCNF/BA25, and starch/LCNF/BA50, respectively. This indicates that the film color shifted from a bluish tone to a yellowish tone as the pH increased from 2 to 13. Similarly, an intelligent film developed using potato starch and blueberry anthocyanin copigmented with ferulic acid recorded b^* values of the film as −2.57 at pH 2 and increased to −0.09 at pH 8.[30] Fig. 4(d) compares the color parameters (ΔE) of the films across the pH range of 2 to 13. In the pH range above 3, all BA-containing films exhibited ΔE values ≥2, the recognized threshold for a visible color change detectable by the human eye.[31] Notably, the starch/LCNF/BA50 films showed significantly higher ΔE values than STARCH/LCNF/BA10 films at the same pH levels. In the alkaline range, ΔE values for starch/LCNF/BA50 exceeded 15, indicating very distinct color differences easily noticeable without instruments. The mechanism behind the color change in starch/LCNF/BA films could be due to BA structurally changing from flavonoid cations to quinone-type

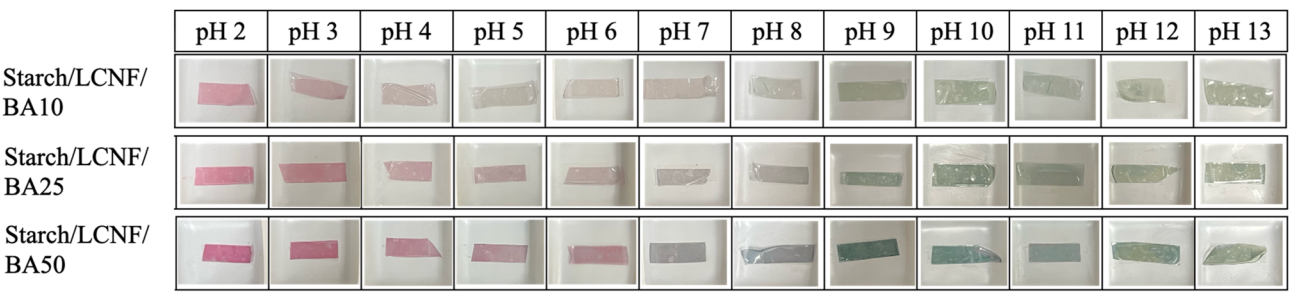

Fig. 3 Pictures of starch/LCNF film with 10%, 25%, and 50% BA showing color change when exposed to different pH levels.

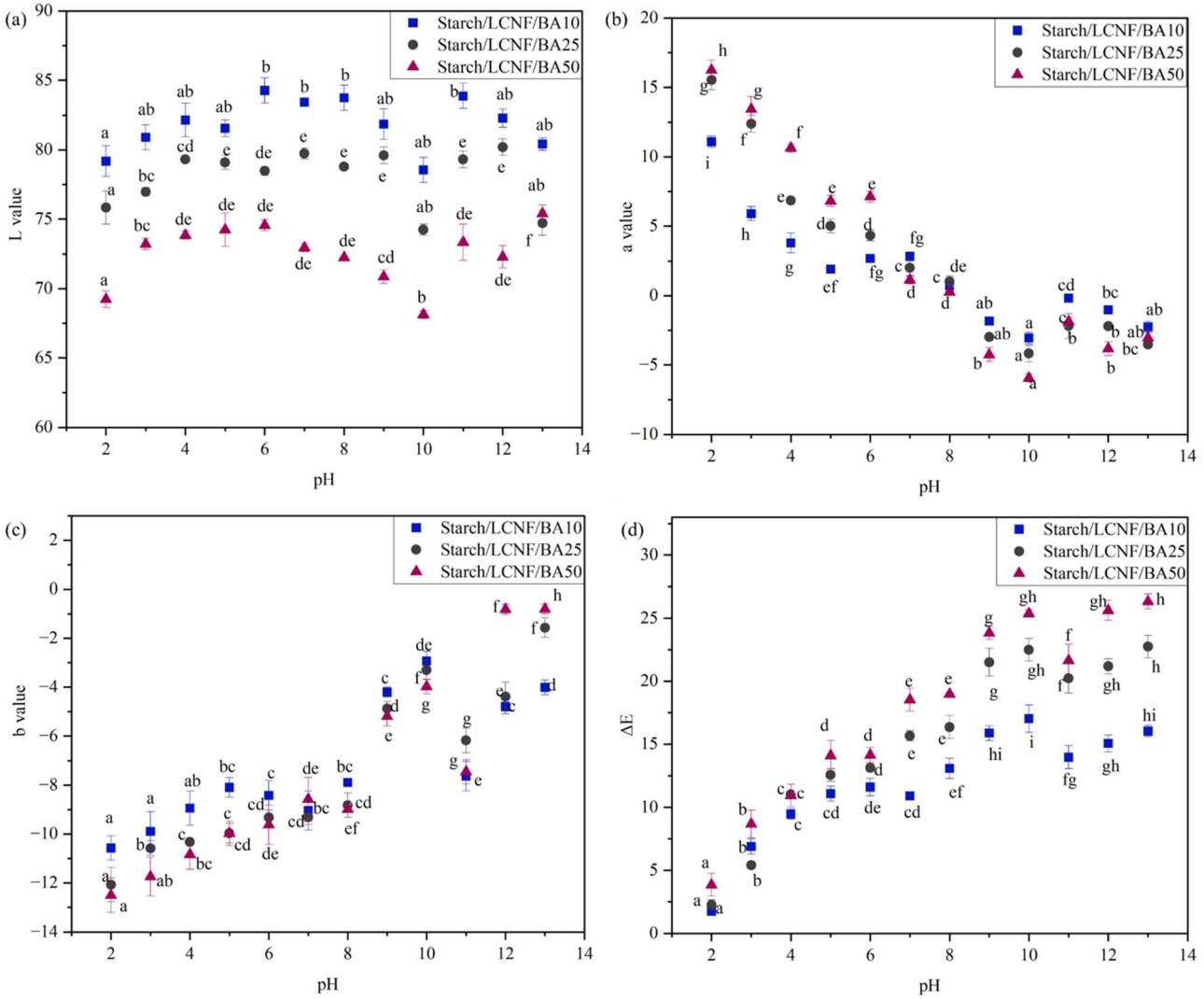

Fig. 4 Color parameters *L* value (a), *a* value (b), *b* value (c) and Δ*E* (d) of starch/LCNF/BA0, starch/LCNF/BA25 and starch/LCNF/BA50.

bases and finally to chalcones; therefore, starch/LCNF/BA10, starch/LCNF/BA25, and starch/LCNF/BA50 films displayed notable color shifts over the pH range. This reaction results in a color change of the film from red-pink to the green-yellow spectrum.[32] The results imply that starch/LCNF/BA50 films have the potential for application as pH indicators for monitoring food freshness.

While the starch/LCNF/BA films exhibited strong pH responsiveness, particularly the BA50 formulation, the color change at neutral to slightly acidic pH (pH 5–7) was relatively subtle compared to the more pronounced shift under strongly acidic or alkaline conditions. This indicates a limitation in detecting early-stage spoilage where pH changes may be minor. To address this, co-pigmentation strategies, such as combining anthocyanins with natural copigments like ferulic acid or flavonoids, could be employed. Co-pigmentation can enhance color stability and amplify the visual response over narrower pH ranges, improving sensitivity in real-time freshness monitoring. Incorporating co-pigmentation in future formulations may therefore provide a more distinct and early-detectable colorimetric response.

3.3. Morphology of film

The diameter of the isolated LCNF from peach pits was measured using the ImageJ software. The mean diameter of the LCNF was evaluated by analyzing transmission electron microscopy images to record 30 measurements and calculating their average. It ranged from 4 to 5 nm, and its morphology, an interconnected cobweb-like structure, was observed (Fig. S1). The crystallinity index of LCNF was recorded as 42.25% using the Segal method. The influence of incorporating BA into starch–LCNF films on the surface morphology was examined by SEM (Fig. 5). The starch/LCNF/BA0 film showed a smooth and compact surface with homogenous dispersion of LCNF and glycerol. However, few agglomerations were observed, which could be due to starch gel lump or cluster formation due to lignin.[33,34] With the incorporation of BA into the polymer matrix, the surface roughness increased. This could be due to

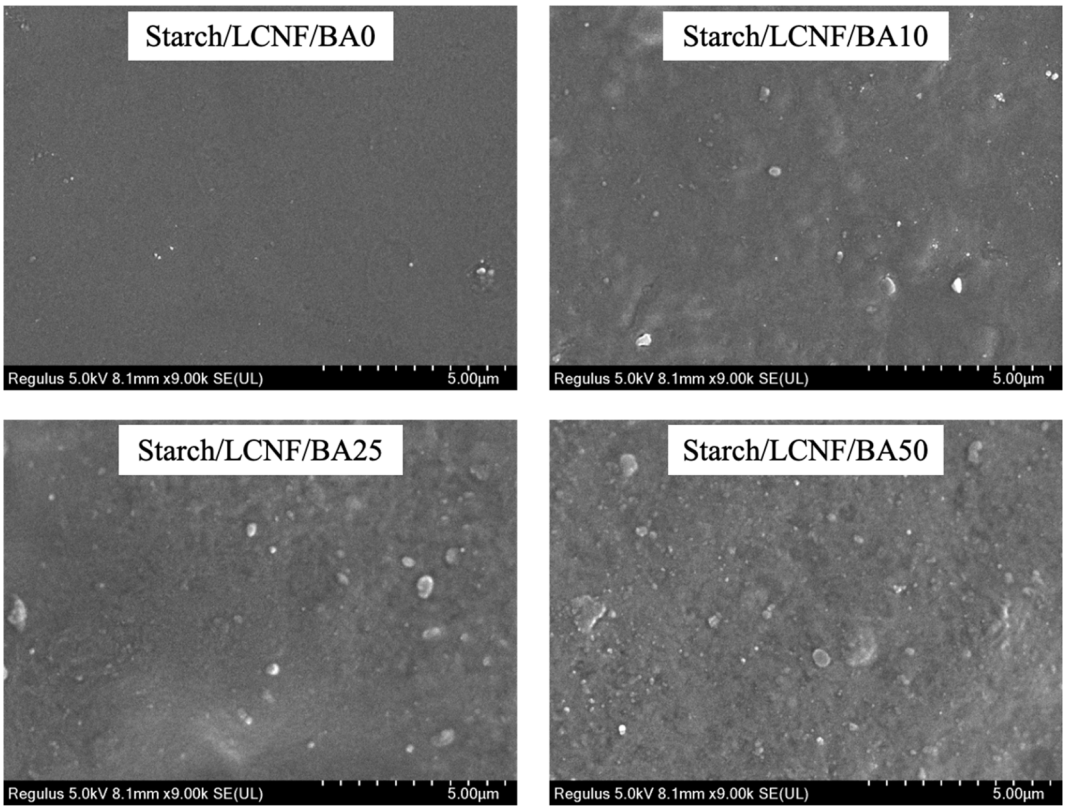

Fig. 5 The SEM images representing surface morphologies of samples: starch/LCNF/BA0, starch/LCNF/BA10, starch/LCNF/BA25 and starch/LCNF/BA50.

the breaking of intermolecular bonds in starch molecules due to the presence of anthocyanin.[35] And as the concentration of BA increased from 10% to 50%, a slight increase in roughness was observed, likely due to the development of a more porous structure. Incorporation of anthocyanin might hinder the hydrogen bond formation between starch and LCNF due to the ring structure of anthocyanin. Similar morphological changes were recorded when anthocyanin was incorporated into polylactic acid and cellulose nanofiber (CNF) matrix.[36] The SEM images of pH-sensitive film made using *Dioscorea zingiberensis* starch and anthocyanin extracted from butterfly pea showed that incorporation of 2% and 3% of anthocyanin resulted in a smooth surface with homogenous dispersion of anthocyanin in the films, and on an increase in the concentration to 4% of anthocyanin, aggregation was observed.[37] Additionally, a film composed of CNF and cellulose nanocrystals (CNC) incorporated with anthocyanin from red cabbage extract demonstrated higher porosity at 50% anthocyanin concentration compared to 20%, attributed to new hydrogen bond formation between anthocyanins and cellulose chains.[38] Thus, it can be stated that the incorporation of BA into the starch/LCNF matrix resulted in morphological changes on the surface of the film.

3.4. Structural changes in film

The molecular cross-linking and structural changes in the films are clearly reflected in the FTIR spectra (Fig. 6). For the control film, the peaks at 3298 cm^{-1} correspond to –OH stretching vibration of the intramolecular and intermolecular hydrogen bonding between the bound water and the glucose molecule present in starch.[39] The peaks at 2933 cm^{-1} and 1150 cm^{-1} may be attributed to the stretching of the C–H bond and the stretching of the C–O bonds in the pyranose ring of the glucose monomer, respectively.[40] The bands between 994 cm^{-1} and 1079 cm^{-1} were identified as corresponding to the pyranose ring found in the glucose residues of the starch.[41] The characteristic cellulose peak was detected in all the samples due to the presence of LCNF at 1417 cm^{-1} which is due to CH_2 bending vibration, 1328 cm^{-1}, which is due to the C–O stretching vibration, the phenol or alcohol vibrations are represented at 1150 cm^{-1}, the C–O bond is assigned to 1018 cm^{-1} and the C–O–C stretching vibration at the β-glycosidic bond is assigned to 850 cm^{-1}.[42,43] The observed similarity between cellulose and starch peaks is attributed to their comparable chemical structures.[44]

The characteristic peaks of BA were observed at 3294 cm^{-1}, attributed to the –OH stretching, 1639 cm^{-1} due to the C=C vibration of the aromatic ring skeleton, and 1448 cm^{-1} due to the C=O stretching vibration, corresponding to the flavonoid structure in anthocyanins.[45] The peak at 1155 cm^{-1} is attributed to the stretching vibration of phenolic C–O, and the peak at 1041 cm^{-1} corresponds to C–H deformation of the aromatic ring.[31,46]

The band corresponding to –OH stretching vibrations of the film samples exhibits a hypsochromic shift from 3298 to

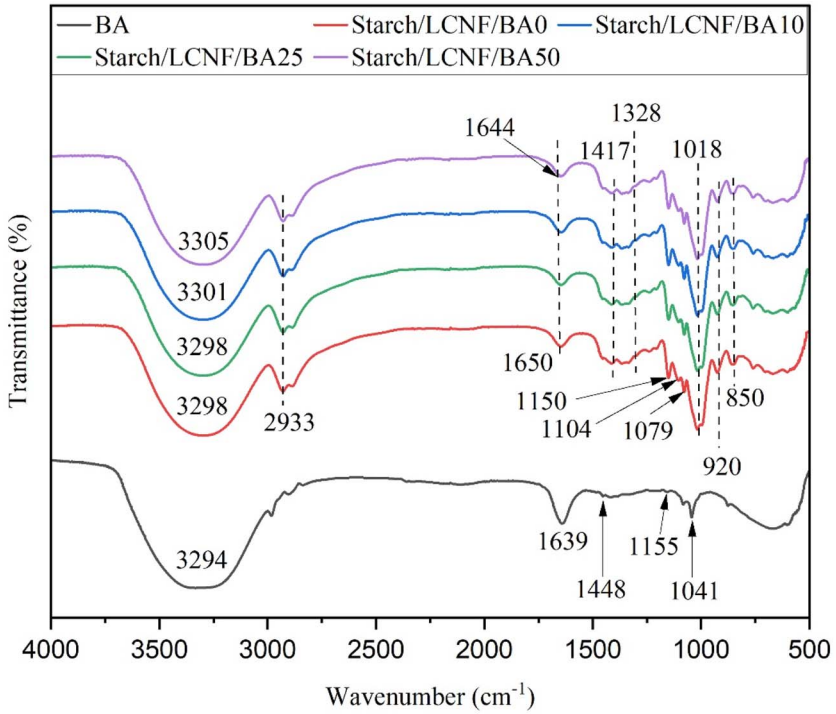

Fig. 6 The FTIR spectra representing structural changes in samples: starch/LCNF/BA0, starch/LCNF/BA10, starch/LCNF/BA25 and starch/LCNF/BA50.

3305 cm^{-1} and a bathochromic shift from 1650 cm^{-1} to 1644 cm^{-1} after BA addition, revealing hydrogen bonding between BA and starch/LCNF. However, the position of the distinctive peaks was not significantly affected by the presence of BA in the films. This could be attributed to the relatively low concentration of BA in films, which was insufficient to cause a noticeable peak shift. Furthermore, it was demonstrated that the pH-sensitive film configuration remained unaffected by changes in BA concentration, consistent with previously reported findings. A starch and poly(butylene adipate-*co*-terephthalate) (PBAT) matrix was incorporated with blueberry extract to develop a pH-sensitive film using the extrusion method. FTIR results showed no significant change in the intensity of blueberry extract peaks.[3,47] Some of the peaks, such as 1448 cm^{-1} and 1041 cm^{-1} disappeared after incorporation of the BA into the starch/LCNF. The disappearance of peaks at 1442 cm^{-1} and 1268 cm^{-1} was recorded in a film composed of casein and carboxymethyl cellulose incorporated with anthocyanin.[46] Therefore, it can be concluded that the addition of anthocyanin did not substantially alter the structural bonding of the starch and LCNF composite films.

3.5. Thermal analysis

The thermal degradation behavior of the films with varying BA levels occurred in three distinct stages, as shown in Fig. 7(a). The initial peak, ranging from 30 °C to 185 °C, could be attributed to the vaporization of the films' low-molecular-weight compounds (including residual moisture and glycerol) and bound water. During this phase, approximately 9% to 20% of total weight was lost.

Films containing BA exhibited greater weight loss, ranging between 10 and 14% compared to the control films (9%), likely due to the disruption of intermolecular hydrogen bonds between starch and LCNF caused by the presence of BA at the elevated temperature. With increasing BA concentration, weight loss increased at this stage; however, the weight loss for starch/LCNF/BA50 samples (13%) was lower than that for starch/LCNF/BA25 samples (14.3%), which could be due to the slightly better intermolecular bonding in the film matrix and BA concentration. As mentioned by Cai *et al.*, 2020, the maximum weight loss temperature for anthocyanins is near 130 °C, where deglycosylation and ring-opening processes occur, leading to the breakdown of anthocyanins into phenolic acids and aldehydes.[48] These interactions may have facilitated faster water vaporization and the early breakdown of starch and LCNF structures. Similar thermal behavior was observed in cassava starch films incorporated with anthocyanins extracted from black plum peel.[49]

The second stage of weight loss, occurring between 185 °C and 266 °C, is primarily attributed to the thermal decomposition of glycerol. At the second stage, 9% to 12% of the weight occurs. Similarly, cassava starch matrix incorporated with Chinese bayberry anthocyanin showed a weight loss of approximately 10% in the temperature range of 185–260 °C due to the evaporation of glycerol.[50]

The third stage, which ranged from 266 °C to 360 °C, was triggered by the removal of polyhydroxyl groups from starch, as well as the depolymerization and breakdown of the starch matrix. During this stage, the overall weight loss ranged between 44% and 65%. In the temperature range of 300–390 °C,

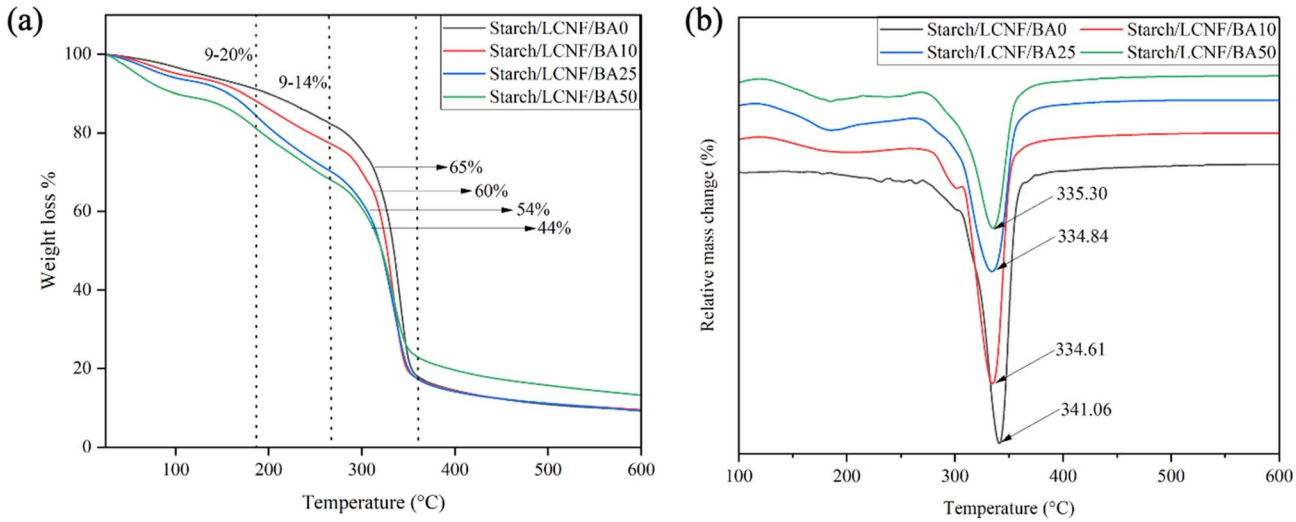

Fig. 7 The TGA (a) and DTG (b) curves of starch/LCNF/BA0, starch/LCNF/BA10, starch/LCNF/BA25 and starch/LCNF/BA50 film samples.

significant weight loss of approximately 30% in sweet potato starch and purple sweet potato anthocyanin film occurred due to hydroxyl dehydration.[22] Interestingly, the anthocyanin-containing films exhibited approximately 21% less weight loss compared to the control film. This suggests that the presence of anthocyanins enhances thermal stability at higher temperatures by forming additional interactions within the polymer matrix that slow down decomposition.

Once 500 °C is reached, the weight percentage stays essentially unchanged, indicating that all volatile substances have been eliminated and that only the residue is left. Among all the film samples, starch/LCNF/BA50 showed the highest residual weight of 13% at 600 °C, indicating better thermal stability compared to other films. Similar results were reported by Hasan *et al.*, 2025, who found that films made from sweet potato starch and chitosan nanoparticles incorporated with anthocyanins from purple sweet potato reported a residual weight at 600 °C of 38%, whereas the control film showed only 13%, indicating enhanced thermal resistance due to the presence of anthocyanins.[51] On the contrary, the incorporation of *Lycium ruthenicum* anthocyanins into cassava starch film did not show any significant changes in the thermal stability of the films.[52]

The DTG curve peaks suggest the maximum weight loss rate of the film samples. The DTG curve (Fig. 7(b)) showed that the incorporation of anthocyanin influenced the maximum weight loss rate of the films. The DTG peak temperature of the starch/LCNF/BA0 was recorded as 341 °C, which was higher than starch/LCNF/BA10 (334.61 °C), starch/LCNF/BA25 (334.84 °C) and starch/LCNF/BA50 (335.30 °C). The interaction between the polymer matrix and anthocyanin may explain these results. A similar decrease in DTG peak temperature was observed when sweet potato starch was incorporated with 2% of anthocyanin. The DTG peak temperature decreased from 356.83 °C to 354.71 °C.[22] A pH-sensitive film made from starch containing 30% amylose and 0.1 g of red cabbage anthocyanin exhibited comparable degradation behavior. The starch film exhibited a DTG peak temperature of 302.6 °C, which decreased to 292.7 °C upon the incorporation of anthocyanin.[29]

Overall, the incorporation of anthocyanin into starch and LCNF matrix showed a slight decrease in thermal stability due to the presence of anthocyanin, which interrupted the bonding between the starch and LCNF matrix.

3.6. Water barrier property

Films used for food packaging should effectively prevent moisture permeation between the food and its surroundings to maintain food quality. Therefore, minimizing WVTR of the films is essential for their practical application in food packaging. Based on the data shown in Table 2, the starch/LCNF/BA0 film exhibited the lowest WVTR of 156.43 g per 100 inch^2 per day. Upon incorporating 10%, 25%, and 50% of blueberry anthocyanins (BA), the WVTR values increased to 186.31, 189.98, and 194.60 g per 100 inch^2 per day, respectively. This increase can be attributed to a reduction in the structural compactness of the films and the formation of a more porous surface, which enhances the permeability of water molecules through the film. These findings are consistent with SEM results, which indicate that the addition of BA resulted in an irregular and rougher surface morphology. Similarly,

Table 2 WVTR and AOA of control and pH-sensitive films[a]

Samples	WVTR (g per 100 inch^2 per day)	AOA (%)
BA	—	57.92 ± 0.1^{e}
Starch/LCNF/BA0	156.43 ± 3.51^{a}	44.39 ± 0.1^{a}
Starch/LCNF/BA10	186.31 ± 6.66^{b}	47.75 ± 0.1^{b}
Starch/LCNF/BA25	189.98 ± 5.81^{b}	51.45 ± 0.1^{c}
Starch/LCNF/BA50	194.60 ± 4.88^{b}	52.75 ± 0.1^{d}

[a] Values with subscripts a, b, c and d in the above table signify the significant difference at $p < 0.05$.

cornstarch and polyvinyl alcohol composite films were incorporated with anthocyanin extracted from purple sweet potatoes. Water vapor permeability (WVP) of the film was increased from 21×10^{-11} g m^{-1} s^{-1} Pa^{-1} to 23×10^{-11} g m^{-1} s^{-1} Pa^{-1} by the addition of 1% of anthocyanin from purple sweet potato.[53] On the contrary, incorporation of purple sweet potato anthocyanin into sweet potato starch showed a decrease in WVP by 58%.[22] The well-dispersed extracts may function as ultra-fine fillers, increasing the tortuosity of the permeability channel for water vapor, and the incorporation of extracts may increase the surface hydrophobicity, which delays the dissolution of water molecules.[3] Overall, the current findings suggest that while BA incorporation enhances the visual and functional responsiveness of the starch/LCNF films, it also compromises their water barrier properties by increasing moisture permeability. The acceptable WVTR for food packaging, often measured at 100 °F (37.8 °C) and 90% RH, typically ranges from 0.001 to 10 g per 100 inch^2 per day. Commercialization of anthocyanin-based pH-sensitive films for intelligent packaging is still a new technology facing challenges. Therefore, future developments include studying its performance under varying humidity conditions and improving its hydrophobicity.

3.7. Mechanical strength

The mechanical characteristics of food packaging films demonstrate their capacity to maintain sustainability and high integrity throughout the food supply chain, as determined by measuring tensile strength, elongation at break, and Young's modulus (Fig. 8). Tensile strength of starch/LCNF/BA0 was recorded as 31.88 MPa, and with the addition of 10% of BA, there was a noticeable decrease in the tensile strength (3.81 MPa). This may be attributed to the way anthocyanin molecules hinder the interactions between starch and LCNF, leading to a decrease in the film's tensile strength.[54] Tensile strength of cassava starch on incorporation of anthocyanin was decreased from 5.7 MPa to 3.8 MPa.[16] This could be due to the extract's poor interactions with starch, LCNF, and glycerol, resulting in a heterogeneous and discontinuous film structure, as observed in the SEM images. In contrast, Mu *et al.* (2025) reported an increase in tensile strength from 0.1 MPa to 1.1 MPa when BA was added to a hydroxypropyl methylcellulose, gelatin, and κ-carrageenan composite, which could be due to the compatibility between the polymer matrix and anthocyanin, which improved the compactness of the film.[24]

Elongation at break (EAB) for the starch/LCNF/BA0, starch/LCNF/BA10, starch/LCNF/BA25, and starch/LCNF/BA50 films was recorded as 2.19%, 15.33%, 29.39%, and 25.68%, respectively. The progressive increase in EAB with higher concentrations of BA suggests enhanced film flexibility, likely due to the plasticizing effect of anthocyanins and their ability to disrupt the tightly packed polymer chains. This facilitates increased molecular mobility and elasticity within the starch/LCNF matrix. However, a slight decline in EAB at the highest concentration (50%) may indicate the onset of saturation or possible phase separation, which could hinder uniform stress distribution. A similar trend was observed by Nandi and Guha (2024), where the addition of 2% betel leaf petiole extract to potato starch films increased EAB from 9% to 20%, supporting the role of plant-based polyphenols in enhancing film flexibility.[55]

Young's modulus decreased significantly with BA incorporation, from 2227.93 MPa for starch/LCNF/BA0 to 286.59 MPa for starch/LCNF/BA50. This reduction indicates a softer and more ductile material, aligning with the increased EAB. Similar results were reported when sago starch was incorporated with *Brassica oleracea* anthocyanin, which showed a decrease in Young's modulus from 210 to 175.[56] Thus, it can be stated that the incorporation of BA resulted in a significant change in the starch and LCNF-based film matrix, leading to a decrease in tensile strength and Young's modulus, but an increase in EAB.

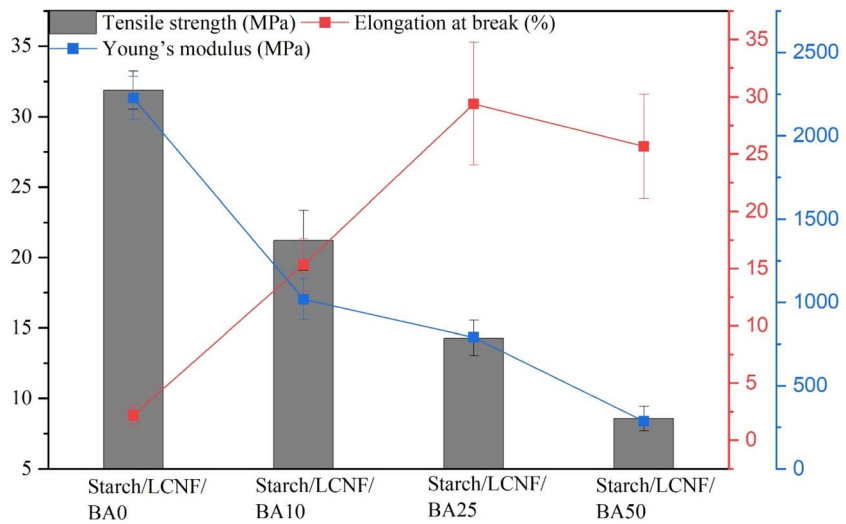

Fig. 8 Tensile strength, elongation at break and Young's modulus of starch/LCNF/BA0, starch/LCNF/BA10, starch/LCNF/BA25 and starch/LCNF/BA50 film samples.

The acceptable tensile strength and Young's modulus range for PLA-based film manufactured in the industry typically range between 39.9–52.2 MPa and 3300–3500 MPa, respectively.[57,58] For the commercial production of starch/LCNF/BA-based film, the mechanical properties need to be further improved to meet the acceptable level.

3.8. Antioxidant activity

Table 2 presents the antioxidant scavenging properties of BA extract and the prepared pH-sensitive films. The DPPH scavenging activity of BA was recorded as 57.8%. The minimum antioxidant activity was recorded for the starch/LCNF/BA0 film sample (44.39%), and the highest was recorded for the starch/LCNF/BA50 sample (52.95%). Starch/LCNF/BA0 itself exhibited antioxidant activity due to the presence of lignin, which has an aromatic structure acting as an antioxidant agent, thereby preventing or retarding oxidation processes induced by oxidizing species. Incorporation of 7% of LCNF isolated from wheat straw into the PVA matrix showed an increase in antioxidant power from 4.8% to 10% due to the presence of residual lignin.[59] Specifically, increasing the anthocyanin content from 10% to 50% raised the antioxidant activity from 44.39% to 52.75%. This improvement is attributed to the strong electron-donating ability of phenolic hydroxyl groups in anthocyanins, which effectively trap free radicals and interrupt chain reactions, making polyphenolic compounds excellent nucleophiles.[3] Mu and his colleagues found that the anthocyanins enhance antioxidant activity by contributing to the conjugated π-electron system, which effectively scavenges free radicals. They reported that incorporating 8% blueberry extract into a composite film made of hydroxypropyl methylcellulose, gelatin, and κ-carrageenan increased its antioxidant activity from 20% to 86%.[24] Compared with the literature, the antioxidant activity of starch/LCNF/BA films was lower than previously reported. This could be due to the exposed temperature during the film-forming solution, which would have impacted anthocyanin degradation rates.[60] Some studies have used purified anthocyanin extracts, which explains the higher antioxidant activity in the resulting films. Similar results have been reported in earlier studies in which red cabbage anthocyanins were added to composite films of cellulose nanocrystals and nanofibrillated cellulose. The antioxidant capacity of films with 20, 30, 40, and 50 wt% of extract was 60%, 80%, 91%, and 92%, respectively.[61] These results collectively indicate that incorporating blueberry anthocyanins into starch and LCNF polymer matrices significantly enhances the antioxidant properties of the films to around 53%.

3.9. Application of starch/LCNF/BA film in monitoring the freshness of chicken

To evaluate the practical performance of the pH-sensitive films, the starch/LCNF/BA50 film, chosen for its high Δ*E* values and

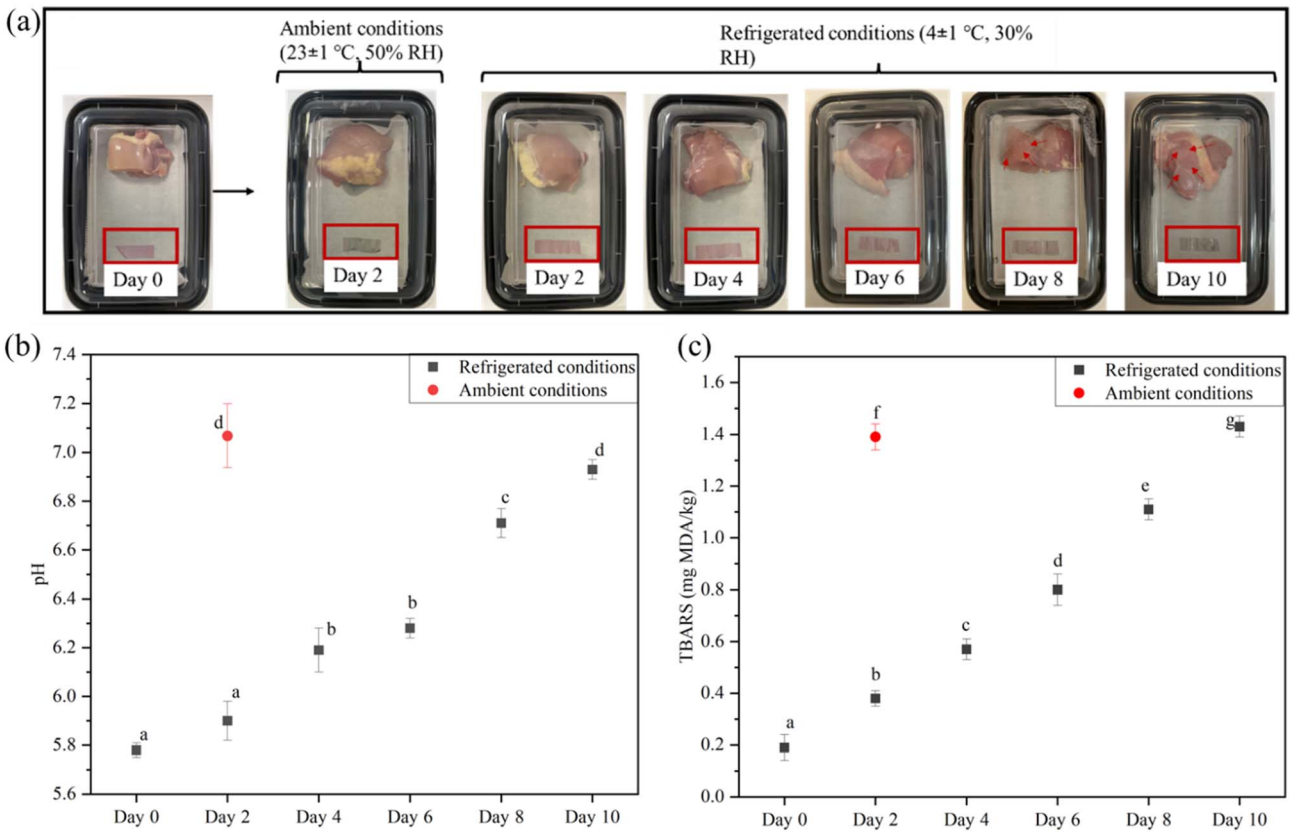

Fig. 9 (a) Picture, (b) pH values and (c) TBARS values of the chicken stored at 4 ± 1 °C, 30% and 23 ± 1 °C, 50%.

visibly detectable color changes, was selected to monitor the freshness of fresh chicken stored at 4 °C (30% RH) and 23 °C (50% RH), as illustrated in Fig. 9(a). The starch/LCNF/BA50 film exhibited a noticeable color change after 24 hours when used to monitor chicken stored at 23 °C, likely due to a pH increase within the chicken, signaling spoilage. In contrast, chicken stored at 4 °C caused no significant color change in the film on day 1. However, by day 5, the film began to darken, and by day 9, it had shifted to a grayish-purple hue. Similarly, Gao *et al.*, 2024 reported that a starch/PBAT/blueberry extract film used as a spoilage indicator for shrimp changed color from purple (day 0) to grey (day 8), demonstrating comparable effectiveness in detecting food spoilage.[3]

The two key metrics used to assess the freshness of chicken are pH measurement and thiobarbituric reactive substances (TBARS), which can help compare the effectiveness of the starch/LCNF/BA50 film in preventing spoilage.

Meat and fish spoil primarily due to microbial spoilage, lipid oxidation and enzymatic breakdown of proteins, producing volatile compounds such as amines, ammonia and aldehydes that increase the pH inside the packaging.[62] The pH of fresh chicken was recorded as 5.78 and increased to 7.07 on day 2 (at 23 °C), then gradually increased to 6.93 on day 10 (at 4 ± 1 °C), as shown in Fig. 9(b). Similar results were obtained for chicken breast stored at 4 ± 1 °C, allowing for the observation of the pH sensitivity of a film composed of gelatin, sodium alginate, and plum peel extract. The chicken breast increased their pH from 5.82 (day 0) to 6.84 (day 10).[63] The pH value of chicken above 6.7 is considered spoiled.[64] This suggests that the chicken samples remained in a consumable state until day 6, as indicated by the color of starch/LCNF/BA50. On day 8, the pH was around 6.71, indicating spoilage, which was also evident from the change in film color. TBARS values are commonly used to measure lipid oxidation, a key factor affecting meat quality. Although there is no official regulatory limit for TBARS concentration in meat, values above 0.5 mg kg^{-1} indicate the onset of oxidation, often associated with rancid flavors, while levels exceeding 1.0 mg kg^{-1} are generally considered unacceptable for consumption.[65]

During storage, fat oxidation generally occurs and subsequently triggers decomposition, resulting in the production of aldehydes and ketones, along with an increase in the TBARS content.[66] As shown in Fig. 9(c), the TBARS value of the chicken on day 0 was recorded as 0.19 mg MDA per kg. On day 2, the TBARS value for chicken stored at 4 ± 1 °C and 23 ± 1 °C was recorded as 0.38 mg MDA per kg and 1.11 mg MDA per kg, respectively. TBARS value for chicken stored at 4 ± 1 °C gradually increased and reached 1.43 mg MDA per kg on day 10, which also showed changes in the starch/LCNF/BA50 film color to grayish purple. A composite film composed of starch, gellan gum, sodium carboxymethyl cellulose, nisin, and anthocyanin was used to study the pH sensitivity of chicken breast samples stored at 4 ± 1 °C. The TBARS value showed an increase from 0.19 mg MDA per kg (day 0) to 1.71 mg MDA per kg (day 12).[67]

The breakdown of fat, protein, and carbohydrates in chicken produces aldehydes, ketones, alcohols, and volatile compounds, which influence both pH and TBARS values and consequently alter the color of the film. These findings demonstrate that the starch/LCNF/BA50 pH-sensitive film can serve as an effective tool for real-time monitoring of the freshness of meat and seafood products.

4. Conclusion

Blueberry extract was successfully extracted and incorporated into the starch/LCNF matrix, as confirmed by FTIR, indicating good compatibility. The observation of colorimetric changes following the immersion of starch/LCNF-based composite films incorporating BA into buffer solutions with varying pH values demonstrated the potential of an intelligent packaging system. Overall color difference values (ΔE^*) more than 3 were found in the starch/LCNF/BA50 film samples, indicating that the color variations are visible to the naked eye. In the pH range of 2 to 13, the color changes of films containing BA varied from red to green. The findings have shown that the addition of BA impacts the physicochemical characteristics and structure of film samples. Chicken stored at 4 ± 1 °C, 30%, and 23 ± 1 °C, 50%, showed changes in film color from reddish pink to grayish purple, corresponding to changes in pH and TBARS value. To improve the stability, sensitivity and resolution of color change within this narrow pH range for intelligent packaging, these developed films need to be studied for co-pigmentation. Therefore, the starch/LCNF/BA50 film has great potential application as a pH-sensitive film, and the color changes of the film can easily indicate the freshness and quality of chicken at ambient and chilled temperatures. In future work, incorporating a hydrophobic component could help improve the WVTR, and studying the stability of an anthocyanin-incorporated film would be an essential aspect from a commercialization perspective.

Reflect

This research paper, titled "Lignocellulose nanofibers (LCNFs) reinforced starch-based intelligent film to detect lipid oxidation of chicken breast", has been prepared solely by the author(s), and all contributors have been appropriately credited.

Author contributions

Afreen Sultana: conceptualization, investigation, data curation and writing-original draft and editing; Sneh Bangar: conceptualization, project administration, supervision, and writing-review & editing. Scott Whiteside: funding acquisition, supervision, project administration, writing-review & editing.

Conflicts of interest

The authors declare that there is no conflicts of interest.

Data availability

The data that support the findings of this study are available from the corresponding author upon reasonable request.

Supplementary information (SI) is available. See DOI: https://doi.org/10.1039/d5fb00942a.

References

1 A. B. Amaral, M. V. Da Solva and S. C. D. S. Lannes, *Food Sci. Technol.*, 2018, **38**, 1–15.
2 R. Domínguez, M. Pateiro, M. Gagaoua, F. J. Barba, W. Zhang and J. M. Lorenzo, *Antioxidants*, 2019, **8**, 429.
3 S. Gao, S. Sun, J. Zhao, W. Wang and H. Hou, *Food Chem.*, 2024, **449**, 139217.
4 F. Zeng, Y. Ye, J. Liu and P. Fei, *Food Chem.: X*, 2023, **17**, 100531.
5 Q. Ma, X. Lu, W. Wang, M. A. Hubbe, Y. Liu, J. Mu, J. Wang, J. Sun and O. J. Rojas, *Food Packag. Shelf Life*, 2021, **28**, 100634.
6 Z. Xu, X. Yu, W. Liu, J. Cheng and G. Xiong, *Food Chem.: X*, 2025, **27**, 102487.
7 A. Panwar, S. Kumar, A. Dhiman, V. Kumar, D. Gupta and A. Sharma, *Microchem. J.*, 2024, **207**, 111732.
8 P. S. Kumar, T. Shuprajhaa, A. Rajendran and K. Dhandapani, *Food Packag. Shelf Life*, 2024, **46**, 101375.
9 K. Akhila, D. Ramakanth, L. Lakshman Rao, S. Singh and K. K. Gaikwad, *Sustain. Food Technol.*, 2024, **2**, 860–875.
10 S. K. Mary, R. R. Koshy, J. Daniel, J. T. Koshy, L. A. Pothen and S. Thomas, *RSC Adv.*, 2020, **10**, 39822–39830.
11 C. Duan, X. Xiao, Y. Yu, M. Xu, Y. Zhang, X. Liu, H. Dai, F. Pi and J. Wang, *Food Chem.*, 2024, **431**, 137155.
12 V. Lohachoompol, G. Srzednicki and J. Craske, *J. Biomed. Biotechnol.*, 2004, **2004**, 248.
13 X. Wang, Y. Guo, M. Yuan, Y. Wang, D. Wang, Z. Guo and Z. Wang, *Food Packag. Shelf Life*, 2025, **49**, 101525.
14 C. Shi, J. Zhang, Z. Jia, X. Yang and Z. Zhou, *J. Sci. Food Agric.*, 2021, **101**, 1800–1811.
15 C. L. Luchese, V. F. Abdalla, J. C. Spada and I. C. Tessaro, *Food Hydrocoll.*, 2018, **82**, 209–218.
16 R. Andretta, C. L. Luchese, I. C. Tessaro and J. C. Spada, *Food Hydrocoll.*, 2019, **93**, 317–324.
17 M. Meenu, A. K. Pujari, S. Kirar, Mansi, A. Thakur, M. Garg and J. Bhaumik, *Sustain. Food Technol.*, 2025, **3**, 414–424.
18 A. Heydarian and N. Shavisi, *Food Packag. Shelf Life*, 2023, **40**, 101219.
19 Y. Palanisamy, V. Kadirvel and N. D. Ganesan, *Sustain. Food Technol.*, 2025, **3**, 161–180.
20 S. Punia Bangar, W. S. Whiteside, K. D. Dunno, G. A. Cavender, P. Dawson and R. Love, *Int. J. Biol. Macromol.*, 2022, **203**, 350–360.
21 A. Sultana, S. P. Bangar, K. Dunno and W. S. Whiteside, *Int. J. Biol. Macromol.*, 2026, 151528.
22 M. Sohany, I. S. M. A. Tawakkal, S. H. Ariffin, N. N. A. K. Shah and Y. A. Yusof, *Foods*, 2021, **10**, 2005.
23 F. Hu, Y. Z. Song, K. Thakur, J. G. Zhang, M. R. Khan, Y. L. Ma and Z. J. Wei, *Food Chem.*, 2024, 139676.
24 L. Mu, J. Bi, H. Zhao, J. Li, H. M. Hou, G. L. Zhang, H. Hao and L. Zhou, *Food Chem.: X*, 2025, **28**, 102587.
25 Z. Bian, W. Xu, H. Zhang, M. Shi, X. Ji, S. Dong, C. Chen, G. Zhao, X. Zhuo, S. Komarneni, K. Zhang, Z. Ni and G. Hu, *Int. J. Biol. Macromol.*, 2023, **251**, 126192.
26 M. Zhao, M. Nuerjiang, X. Bai, J. Feng, B. Kong, F. Sun, Y. Li and X. Xia, *Int. J. Biol. Macromol.*, 2022, **216**, 361–373.
27 S. Singh, O. F. Nwabor, D. M. Syukri and S. P. Voravuthikunchai, *Int. J. Biol. Macromol.*, 2021, **182**, 1015–1025.
28 C. Wang, Y. Lu, X. An, Y. Wang, N. Wang, Y. Song, N. Hu and M. Ren, *LWT*, 2024, **200**, 116156.
29 M. Faisal, M. Bevilacqua, R. Bro, H. N. Bordallo, J. J. K. Kirkensgaard, K. H. Hebelstrup and A. Blennow, *Int. J. Biol. Macromol.*, 2023, **250**, 126250.
30 J. Li, Y. Bao, Q. Jiang, B. Wen, L. Wang, Y. He, X. Si and B. Li, *J. Food Eng.*, 2024, **383**, 112241.
31 L. Gao, P. Liu, L. Liu, S. Li, Y. Zhao, J. Xie and H. Xu, *Process Biochem.*, 2022, **121**, 463–480.
32 C. Wang and C. Liu, *Food Bioprocess Technol.*, 2024, **17**, 5312–5323.
33 Y. Zhao, A. Tagami, G. Dobele, M. E. Lindström and O. Sevastyanova, *Polymers*, 2019, **11**, 538.
34 A. P. Travalini, B. Lamsal, W. L. E. Magalhães and I. M. Demiate, *Int. J. Biol. Macromol.*, 2019, **139**, 1151–1161.
35 R. R. Koshy, J. T. Koshy, S. K. Mary, S. Sadanandan, S. Jisha and L. A. Pothan, *Food Control*, 2021, **126**, 108039.
36 X. Cheng, Q. Zhao, J. Kang, X. Zhao, X. He and J. Li, *ACS Appl. Polym. Mater.*, 2023, **5**, 6307–6317.
37 L. Wang, C. Yang, X. Deng, J. Peng, J. Zhou, G. Xia, C. Zhou, Y. Shen and H. Yang, *Int. J. Biol. Macromol.*, 2023, **245**, 125485.
38 M. Shayan, J. Gwon, M. S. Koo, D. Lee, A. Adhikari and Q. Wu, *Cellulose*, 2022, **29**, 9731–9751.
39 M. Cheng, X. Yan, Y. Cui, M. Han, X. Wang, J. Wang and R. Zhang, *J. Food Eng.*, 2022, **321**, 110943.
40 A. Sultana, S. Punia Bangar and W. S. Whiteside, *Biomass Convers. Biorefin.*, 2024, **1–9**, 8745–8753.
41 Y. Qin, Y. Liu, X. Zhang and J. Liu, *Food Hydrocoll.*, 2020, **100**, 105410.
42 E. Kaffashsaei, H. Yousefi, T. Nishino, T. Matsumoto, M. Mashkour and M. Madhoushi, *Waste Biomass Valorization*, 2023, **14**, 2931–2943.
43 S. Fukugaichi, E. Mayasari, E. Johan and N. Matsue, *Chem. Pap.*, 2023, **77**, 3619–3627.
44 E. Malekzadeh, A. Tatari and M. D. Firouzabadi, *Carbohydr. Polym.*, 2023, **309**, 120699.
45 F. Hu, Y. Z. Song, K. Thakur, J. G. Zhang, M. R. Khan, Y. L. Ma and Z. J. Wei, *Food Chem.*, 2024, **453**, 139676.
46 H. Cui, X. Si, J. Tian, Y. Lang, N. Gao, H. Tan, Y. Bian, Z. Zang, Q. Jiang, Y. Bao and B. Li, *Food Hydrocoll.*, 2022, **122**, 107073.
47 S. Tan, C. Zhou, P. Rao, H. Tan and J. Wang, *Meat Sci.*, 2025, **225**, 109808.
48 X. Cai, X. Du, D. Cui, X. Wang, Z. Yang and G. Zhu, *Food Hydrocolloids*, 2019, **91**, 238–245.
49 N. Zhang, P. Tao, Y. Lu and S. Nie, *Cellulose*, 2019, **26**, 7823–7835.

50 D. Yun, H. Cai, Y. Liu, L. Xiao, J. Song and J. Liu, *RSC Adv.*, 2019, **9**, 30905–30916.
51 M. Hasan, A. Utami, C. Siregar, L. Hanum, I. Khaldun and M. Nazar, *Results Eng.*, 2025, **25**, 104448.
52 Y. Qin, Y. Liu, H. Yong, J. Liu, X. Zhang and J. Liu, *Int. J. Biol. Macromol.*, 2019, **134**, 80–90.
53 K. Zhang, T. S. Huang, H. Yan, X. Hu and T. Ren, *Int. J. Biol. Macromol.*, 2020, **145**, 768–776.
54 M. Xu, D. Fang, C. Shi, S. Xia, J. Wang, B. Deng, B. M. Kimatu, Y. Guo, L. Lyu, Y. Wu, F. Cao and W. Li, *Food Hydrocoll.*, 2025, **158**, 110586.
55 S. Nandi and P. Guha, *Food Chem.*, 2024, **431**, 137103.
56 N. H. Che Hamzah, N. Khairuddin, I. I. Muhamad, M. A. Hassan, Z. Ngaini and S. R. Sarbini, *Membranes*, 2022, **12**, 913.
57 G. Gao, F. Xu, J. Xu and Z. Liu, *Materials*, 2022, **15**, 7039.
58 A. Dmitruk, J. Ludwiczak, M. Skwarski, P. Makuła and P. Kaczyński, *J. Mater. Sci.*, 2023, **58**, 1991–2004.
59 E. Espinosa, I. Bascón-Villegas, A. Rosal, F. Pérez-Rodríguez, G. Chinga-Carrasco and A. Rodríguez, *Int. J. Biol. Macromol.*, 2019, **141**, 197–206.
60 K. H. Erna, W. X. L. Felicia, J. M. Vonnie, K. Rovina, K. W. Yin and M. N. Nur'aqilah, *Biosensors*, 2022, **12**, 211.
61 M. Shayan, J. Gwon, M. S. Koo, D. Lee, A. Adhikari and Q. Wu, *Cellulose*, 2022, **29**, 9731–9751.
62 M. Alizadeh-Sani, M. Tavassoli, E. Mohammadian, A. Ehsani, G. J. Khaniki, R. Priyadarshi and J. W. Rhim, *Int. J. Biol. Macromol.*, 2021, **166**, 741–750.
63 K. Chen, J. Li, L. Li, Y. Wang, Y. Qin and H. Chen, *Food Biosci.*, 2023, **53**, 102584.
64 Y. Liu, Y. Yu, Q. Meng, Q. Wei, W. He, Q. Zhao, C. Tang, X. Feng and J. Zhang, *Food Chem.*, 2022, **384**, 132554.
65 K. Zheng, B. Li, Y. Liu, D. Wu, Y. Bai and Q. Xiang, *LWT*, 2023, **176**, 114547.
66 X. Shen, L. Xing, L. Pan, Y. Miao and W. Zhang, *Poult. Sci.*, 2025, **104**, 104999.
67 Y. Wu and C. Li, *Int. J. Biol. Macromol.*, 2023, **232**, 123464.